A FEED-FORWARD COMPENSATOR FOR VIBRATION REDUCTION CONSIDERING MAGNETIC ATTRACTION FORCE IN BEARINGLESS SWITCHED RELUCTANCE MOTORS

Masatsugu Takemoto
Tokyo Institute of Technology, Meguro-ku, Tokyo, JAPAN, takemoto@ee.titech.ac.jp
Akira Chiba
Science University of Tokyo, Noda, Chiba, JAPAN, chiba@ee.noda.sut.ac.jp
Tadashi Fukao
Tokyo Institute of Technology, Meguro-ku, Tokyo, JAPAN, tfukao@ee.titech.ac.jp

ABSTRACT

In switched reluctance motors, rotor eccentricity due to mechanical errors causes large magnetic attraction force acting on rotor in radial direction. This inherent large magnetic attraction force is one of causes of vibration that have come into problems in switched reluctance motors. The proposed bearingless switched reluctance motors can actively compensate the magnetic attraction force by employing radial force for rotor shaft magnetic suspension.

In this paper, a feed-forward compensator for vibration caused by the magnetic attraction force in the bearingless switched reluctance motors is proposed. It is shown in experimental results that the proposed compensator is effective for vibration reduction and stable operation. In addition, the proposed feed forward compensator is found to be also effective for radial vibration suppression in general switched reluctance motors supported by mechanical bearings.

INTRODUCTION

For special environments, conventional switched reluctance motors have superior performance possibility, because of their inherent advantageous features such as fail safe, robustness, low cost and possible operations in high temperatures or in intense temperature variations [1-2]. Moreover, switched reluctance motors have a good possibility as bearingless motors that have combined characteristics of electrical motors and magnetic bearings. As generally known, in switched reluctance motors, significant amount of magnetic attraction is generated in radial direction, because switched reluctance motors generally have short air-gap length in order to effectively produce rotational reluctance torque. It is quite possible to take an advantage of this inherent large magnetic attraction for rotor shaft magnetic suspension.

Therefore, bearingless switched reluctance motors with differential stator winding configuration have been proposed by the principal authors [3-4]. These motors have two kinds of stator windings composed of motor main windings and radial force windings in the same stator to produce radial force that can realize rotor shaft suspension without mechanical contacts. These motors are expected to be suitable for high-speed drives of special environments.

Regardless of the conventional or bearingless switched reluctance motors, rotor eccentricity due to mechanical error causes large magnetic attraction force acting on the rotor in radial direction. This inherent large magnetic attraction force is one of causes of vibration and subsequent noise emission that have come into problems in switched reluctance motors. It is necessary to actively compensate the magnetic attraction force in order to reduce the vibration. However, the conventional switched reluctance motors can not actively compensate the magnetic attraction force. On the other hand, the bearingless switched reluctance motors can actively control the radial force with the function of magnetic bearings. Therefore, it is possible to actively compensate the magnetic attraction force with the radial force without time delay by means of adding a feed-forward compensator in a feedback controller of rotor radial position.

The effect of a feed-forward compensator for vibration was reported in the previous paper [5]. However, the detailed structure is not reported as yet. In this paper, the detailed structure of a feed-forward compensator for vibration caused by the magnetic attraction force in bearingless switched reluctance motors is proposed. In addition, the proposed feed forward compensator is found to be also effective for radial vibration suppression in general switched reluctance motors supported by mechanical bearings.

WINDING CONFIGURATION AND PRINCIPLE OF RADIAL FORCE PRODUCTION

Fig.1 shows the *A*-phase stator winding configuration and the principle of radial force production. The motor main winding N_{ma} consists of 4-coils connected in series. On the other hand, the radial force windings N_{sa1} and N_{sa2} consist of 2-coils, respectively. These coils are separately wound around confronting stator tooth. The *B*- and *C*-phase windings are situated on one third and two thirds rotational position of the *A*-phase, respectively. As the number of stator poles is 12, these three phases are excited for every 15deg. The rotor angular position θ is defined as $\theta = 0$ at the aligned position of the *A*-phase. The rotor angular position θ in Fig.1 is –10deg.

The thick solid lines show the symmetrical 4-pole fluxes produced by the 4-pole motor main winding current i_{ma}. The broken lines show the symmetrical 2-pole fluxes produced by the 2-pole radial force winding current i_{sa1}. It is evident that the flux density in the air-gap 1 is increased. On the contrary, the flux density in the air-gap 2 is decreased. Therefore, this superimposed magnetic field results in the radial force *F* acting on the rotor toward the positive direction in the α-axis. A radial force toward the negative direction in the α-axis can be produced with a negative current i_{sa1}. Moreover, a radial force in the β-axis can be produced by the 2-pole radial force winding current i_{sa2}. Thus, radial force can be produced in any desired direction. Similarly, this principle can be applied to the *B*- and *C*-phases. The radial force can be continuously generated by these three phases for every 15deg, i.e., from the start of overlap and up to the aligned positions.

RELATION BETWEEN MAGNETIC CENTER AND MAGNETIC ATTRACTION FORCE

Rotor eccentricity from magnetic center causes non-uniformity in the magnetic flux distribution. Therefore, magnetic attraction force acts in the direction of rotor eccentric position, because flux density in radially displaced direction is greater than that in opposite direction. It is important to suspend a rotor shaft at the magnetic center not to produce the magnetic attraction force, which causes vibration. For that purpose, it is necessary to measure the accurate radial position of the magnetic center. Fig.2 shows the measurement method of the *A*-phase magnetic center. The process of measurement is as follows.

1. The rotor is hold with fixing apparatus that can gradually move the rotor in the α- and β-directions.
2. The alternating voltage V_{ma} is applied in motor main winding N_{ma}.
3. The induced voltages V_{sa1}, V_{sa2} of the radial force windings N_{sa1}, N_{sa2} are measured, respectively.
4. The rotor is moved at the radial position where the induced voltages V_{sa1}, V_{sa2} become the least. This rotor radial position is the magnetic center.

The *A*-phase magnetic centers are measured eight times during one rotation by aligning the rotor poles 1-8 with the stator pole 1, respectively. Similarly, the *B*- and *C*-phase magnetic centers are measured. Fig.3 shows the measured results of 3-phase magnetic centers plotted in order of rotatory direction. The magnetic centers of a test motor draw the locus in the shape of a circle with

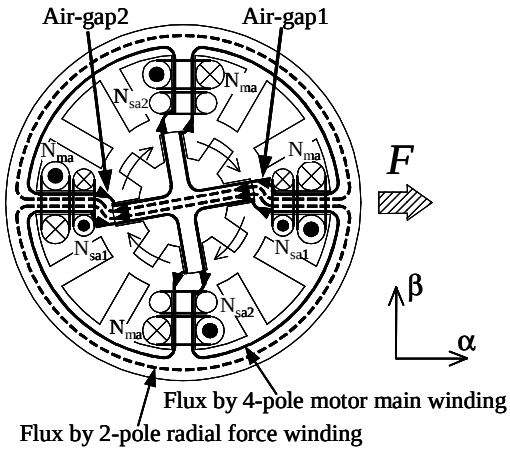

FIGURE 1: *A*-phase winding configuration and principle of radial force production.

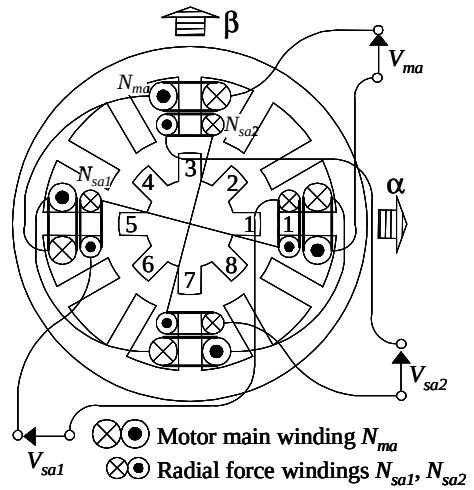

FIGURE 2: Measurement method of magnetic center.

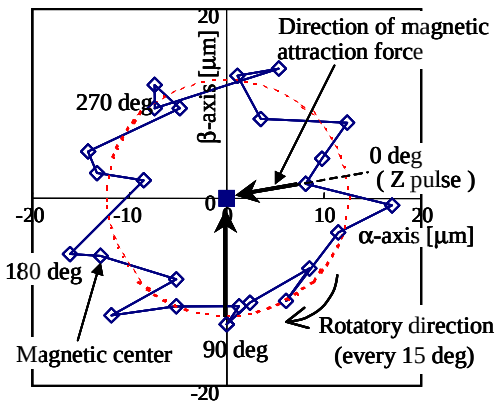

FIGURE 3: Locus of magnetic centers.

the radius of about 13μm. It is desirable to suspend a rotor shaft at the magnetic center in order to minimize the magnetic attraction force. However, if the origin of rotor radial position controller is set at magnetic center of a certain rotor angular position, unbalanced magnetic attraction force is produced at other rotor angular positions. Hence, the origin of rotor radial position controller is set at the central point of the locus of magnetic centers.

A test machine is built. The bottom of rotor shaft is held by the spherical roller bearing, and the rotor shaft is connected with the load machine through the torque meter. In this situation, the rotor radial position is controlled in two axes of α and β. Fig.4 shows the waveforms of rotational speed ω, rotational speed command ω^*, rotor displacements α and β, Z pulse, average torque command $T_{avg}{}^*$, motor main winding current command $i_m{}^*$ on the occasion of the step acceleration with the drive system proposed in [3]. The rotational speed command ω^* is accelerated from 1500r/min to 2500r/min. It is seen that stable operation can be realized at no load. However, the rotor shaft vibrates during the acceleration, that is, high torque period. The magnetic attraction force is constantly produced owing to the gap between the origin of controller and the magnetic centers as shown in Fig.3. Consequently, the vibration of rotor shaft largely appears at the period because the magnetic attraction force is in proportion to the square of air-gap flux density, which is significantly high in high torque generation.

Fig.5 shows the enlarged waveforms during the acceleration. The vibration of rotor shaft exceedingly corresponds to the direction of magnetic attraction force caused by the circular variation of magnetic centers. For example, at rotor angular position θ = 0deg, the origin of controller, i.e., the rotor radial position is situated toward the negative direction in α-axis from the magnetic center. Therefore, the magnetic attraction force acts toward same direction, too. As a result, the rotor shaft is moved toward the negative direction in the α-axis. Similarly, at rotor angular position θ = 90deg, the rotor shaft is moved toward the positive direction in the β-axis, because the origin of controller is situated toward positive direction in β-axis from the magnetic center. It is confirmed that the magnetic attraction force caused by the circular variation of magnetic centers is one of causes of vibration.

THEORETICAL FORMULAE OF MAGNETIC ATTRACTION FORCE

It is necessary to compensate the magnetic attraction force by means of adding a feed-forward compensator considering the locus of magnetic centers in a feedback controller of rotor radial position in order to reduce the vibration without time delay. For that purpose, it is important to derive the accurate theoretical formulae of magnetic attraction force.

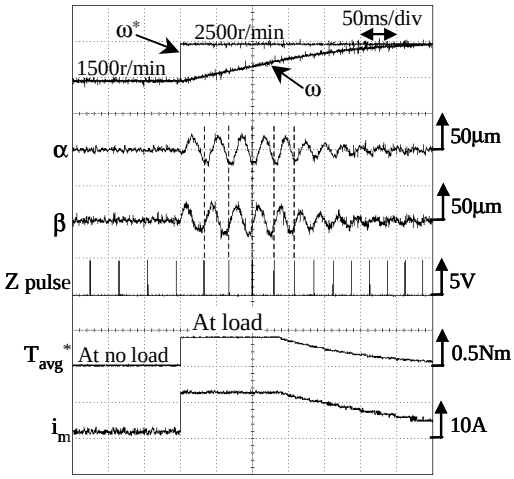

FIGURE 4: Step acceleration with controller neglecting magnetic attraction force.

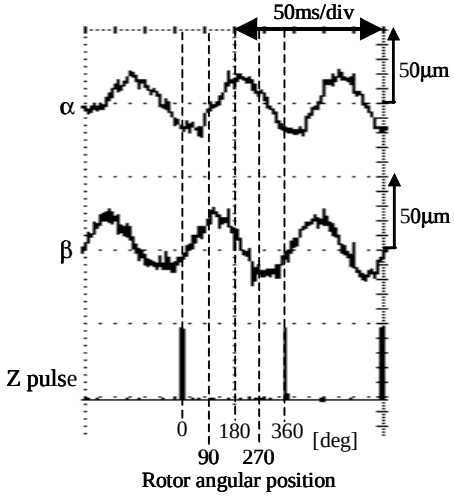

FIGURE 5: Enlarged figure of rotor displacements α, β as shown in Fig.4.

Derivation of Inductances

Fig.6 shows a cross section of the experimental motor coupled with a magnetic equivalent circuit and winding configuration. Voltage sources show magnetomotive forces (MMFs) of the motor main windings and the radial force windings, in addition, permeances P_{a1}~P_{a4}, P_{b1}~P_{b4} of air-gap are expressed as equivalent resistances. Magnetic equivalent circuit of *C*-phase is neglected to have a simple calculation. This is possible because magnetic reluctances of *C*-phase compared with that of *A*- and *B*-phases are extremely large. Only *A*-phase winding configuration, i.e., one phase winding configuration is considered, because two phases is not simultaneously excited. It was proposed in reference [3] that the optimal conduction period is 15deg, that is, one phase excitation is optimal in the drive system with square waveform in motor main winding currents.

If each permeance shown as P_{a1}~P_{a4}, P_{b1}~P_{b4} can be

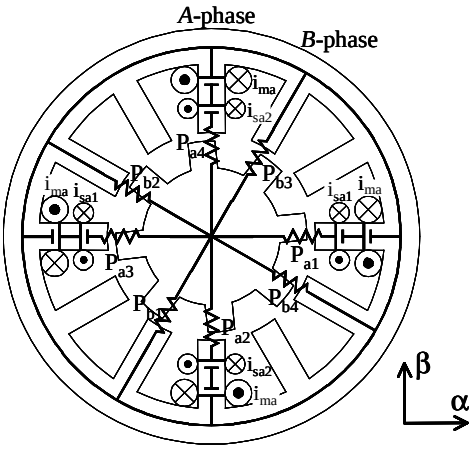

FIGURE 6: A magnetic equivalent circuit .

simply assumed, the self-inductances and the mutual inductances of each winding of *A*-phase can be calculated from Fig.6. It was reported in reference [4] that the radial force caused by superimposing the radial force fluxes on the motor main fluxes is proportional to the derivatives of the mutual inductances. The radial force was minutely derived in reference [4]. On the other hand, the magnetic attraction force is proportional to the derivatives of the self-inductances.

Assumption of Permeances

The permeances P_{a1}~P_{a4}, P_{b1}~P_{b4} can be assumed with the straight magnetic paths only, because the permeance of straight magnetic paths is dominant in the most part of rotor angular position, especially, at the aligned position [4]. To the contrary, it is not necessary to consider the fringing magnetic paths, because the magnetic attraction force is very small at the start of overlap position where the permeance of the fringing magnetic paths is dominant. Accordingly, the permeances P_{a1}, P_{b1} can be derived as,

$$P_{a1} = \frac{\mu_0 hr\left(\frac{\pi}{12} - |\theta_e|\right)}{l_0 - \alpha}. \quad (1)$$

$$P_{b1} = \frac{\mu_0 hr|\theta_e|}{l_0 - \left(-\frac{1}{2}\alpha - \frac{\sqrt{3}}{2}\beta\right)} \quad (2)$$

where, μ_0 is permeability in the air, h is a stack length, r is the radius of the rotor pole, lo is the average air-gap length, θ_e is the rotor angular position from the aligned position of exciting phase. Similarly, P_{a2}~P_{a4}, P_{b2}~P_{b4} can be also derived.

Derivation of Magnetic Attraction force

The self-inductances can be derived from each permeance. The magnetic attraction force is derived from the derivatives of the stored magnetic energy based on the self-inductances with respect to displacements α and β, respectively. The theoretical formulae of the magnetic attraction force of the *A*-phase are written as,

$$F_{um\alpha} = K_{um}(\theta_e)\,\alpha\, i_{ma}^{\,2} \quad (3)$$

$$F_{um\beta} = K_{um}(\theta_e)\,\beta\, i_{ma}^{\,2} \quad (4)$$

$$F_{us\alpha} = K_{us}(\theta_e)\,\alpha\, i_{sa1}^{\,2} \quad (5)$$

$$F_{us\beta} = K_{us}(\theta_e)\,\beta\, i_{sa2}^{\,2} \quad (6)$$

where, $F_{um\alpha}$, $F_{um\beta}$, $F_{us\alpha}$, $F_{us\beta}$, are the magnetic attraction forces produced by i_{ma}, i_{sa1}, i_{sa2} in the α- and β-direction, respectively. $K_{um}(\theta_e)$, $K_{us}(\theta_e)$ are the proportional coefficient of the magnetic attraction force. $K_{um}(\theta_e)$, $K_{us}(\theta_e)$ can be written as,

$$K_{um}(\theta_e) = \frac{N_m^{\,2}\mu_0 hr(\pi - 12|\theta_e|)}{6 l_0^{\,3}} \quad (7)$$

$$K_{us}(\theta_e) = \frac{1}{2}\frac{N_s^{\,2}\mu_0 hr(\pi - 12|\theta_e|)(\pi + 12|\theta_e|)}{6\pi\, l_0^{\,3}} \quad (8)$$

where, N_m is the number of turns of the motor main winding, N_s is the number of turns of radial force winding. Similarly, the magnetic attraction forces of the *B*- and *C*-phases can be also derived. The magnetic attraction forces are proportional to the rotor displacements α, β and the square of stator winding currents, respectively. In addition, if rotor and stator poles are aligned, the magnetic attraction force is maximum. As the rotor rotates from the aligned position, the magnetic attraction force becomes less.

Finite Element Analysis

Fig.7 shows the results of two-dimensional finite element analysis for the magnetic attraction force. Finite element analysis is carried out with the dimensions of the test motor as shown in Table 1 and the following conditions.

(1) The finite element analysis is carried out with respect to the *A*-phase.
(2) The rotor is moved toward the positive direction in the α-axis.
(3) The magnetic attraction forces $F_{um\alpha}$ and $F_{us\alpha}$ are obtained by individually exciting i_{ma} and i_{sa1}, respectively.
(4) The other conditions are shown in Fig.8(a)~(c), respectively.

It is seen that the theoretical formulae are very close to the results of FE analysis for the most part. As the i_{ma} or θ_e increase, the error between the theoretical formulae and the analysis results is gradually increased because of the magnetic saturation. It is evident that the simple theoretical formulae assumed with the straight magnetic paths only are effective for taking account of the magnetic attraction force under unsaturated conditions. The further studies are required to consider the magnetic saturation.

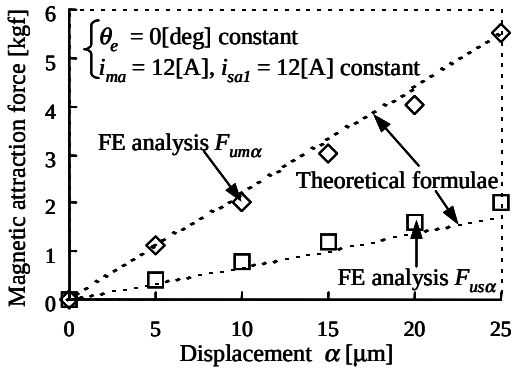

(a) Relationship between α and $F_{um\alpha}$, $F_{us\alpha}$.

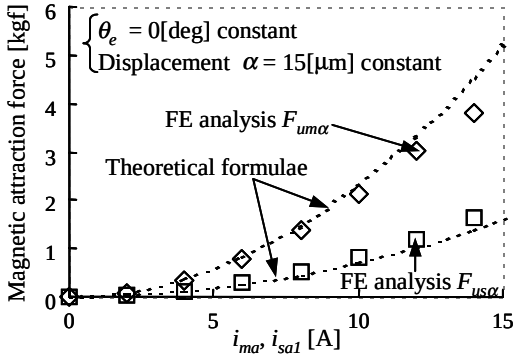

(b) Relationship between i_{ma}, i_{sa1} and $F_{um\alpha}$, $F_{us\alpha}$.

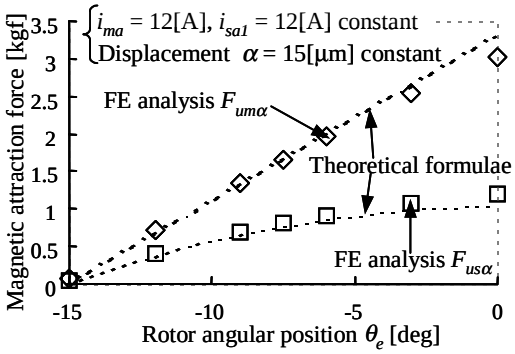

(c) Relationship between θ_e and $F_{um\alpha}$, $F_{us\alpha}$.

FIGURE 7: Magnetic attraction force using FE analysis.

TABLE 1: Dimensions of Test Motor

Number of turns of motor main winding, N_m (0.8 mm ϕ, 3parallels, 1.51mm^2)	14 turns
Number of turns of radial force winding, N_s (0.8 mm ϕ, 2parallels, 1.01mm^2)	11 turns
Arc angle of rotor and stator teeth	15 deg
Stack length, h	50 mm
Outside diameter of stator core	100 mm
Inside diameter of stator pole	50 mm
Radius of rotor pole, r	24.78 mm
Average air-gap length, l_0	0.22 mm

A FEED-FORWARD COMPENSATOR AND EXPERIMENTAL RESULT

It is necessary to add the locus of magnetic centers to (3 – 6) in order to compensate the magnetic attraction force caused by the circular variation of magnetic center. The locus of magnetic centers in Fig.3 is assumed as,

$$\alpha_e = \gamma_e \cos\theta \tag{9}$$

$$\beta_e = -\gamma_e \sin\theta \tag{10}$$

where α_e, β_e are the radial position of the locus of magnetic centers, γ_e is the radius of the locus of magnetic centers, $13*10^{-6}$. The magnetic attraction force considering the locus of magnetic centers can be written by adding (9 – 10) into (3 – 6) as,

$$F_{um\alpha} = K_{um}(\theta_e)(\alpha - \gamma_e \cos\theta)\, i_{ma}{}^2 \tag{11}$$

$$F_{um\beta} = K_{um}(\theta_e)(\beta + \gamma_e \sin\theta)\, i_{ma}{}^2 \tag{12}$$

$$F_{us\alpha} = K_{us}(\theta_e)(\alpha - \gamma_e \cos\theta)\, i_{sa1}{}^2 \tag{13}$$

$$F_{us\beta} = K_{us}(\theta_e)(\beta + \gamma_e \sin\theta)\, i_{sa2}{}^2 . \tag{14}$$

Fig.8 shows the rotor radial position controller adding a feed-forward compensator based on (11 – 14). The feed-forward compensator is the area surrounded with the broken line. If the locus of magnetic centers is any shape except a circle, it is possible to compensate the magnetic attraction force without time delay by means of measuring accurate locus of magnetic centers.

Fig.9 shows the experimental waveforms on the occasion of the step acceleration with the rotor radial position controller adding a feed-forward compensator. The experimental condition is the same as Fig.4. The operation of bearingless switched reluctance motor is stable in spite of the sudden step acceleration. It is found that the proposed feed-forward compensator is extremely effective for the radial position variations caused by the circular variation of magnetic centers.

Applying the proposed feed forward compensator to general switched reluctance motors supported by mechanical bearings is proposed. Fig.10 shows the experimental results of harmonic vibration analysis measured with balance monitor to confirm the effect of the proposed feed forward compensator. The top end of the rotor shaft of a test motor is fixed at $\alpha = 0$, $\beta = 0$ by a mechanical bearing. As mentioned above, the bottom end of rotor shaft is fixed by the spherical roller bearing. In this situation, the test motor is operated as general switched reluctance motors exciting square waveform currents of 12A in motor main windings only. The vibration displacements are measured. Next, the radial force winding currents are additionally excited with the feed-forward compensator only without the feedback controller, i.e., the feedback of rotor displacements. Similarly, the vibration displacements are measured. The rotational speed ω is 1500r/min. The vibration displacements are reduced by actively compensating the magnetic attraction force with the feed-forward compensator. The proposed feed forward compensator

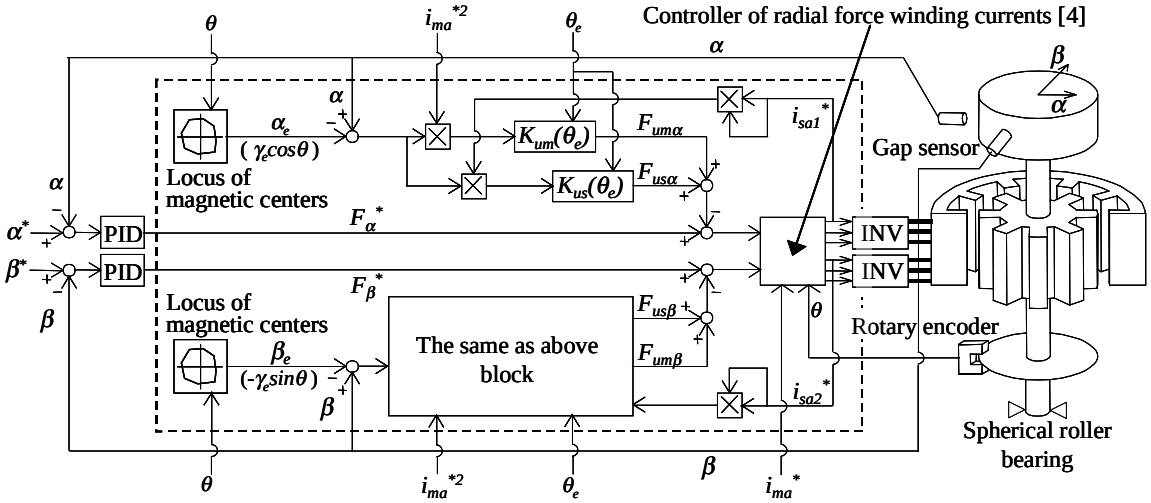

FIGURE 8: Rotor radial position controller adding a feed-forward compensator.

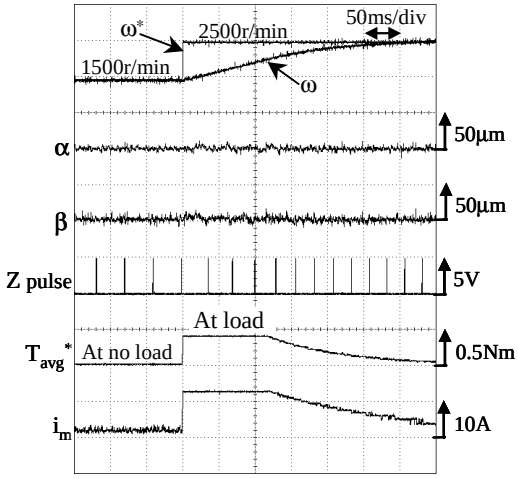

FIGURE 9: Step acceleration with controller considering magnetic attraction force.

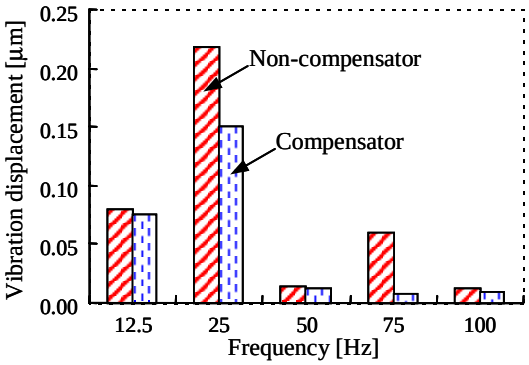

FIGURE 10: Harmonic vibration analysis .

is found to be also effective for radial vibration suppression in general switched reluctance motors supported by mechanical bearings.

CONCLUSION

A feed-forward compensator of the magnetic attraction force considering the locus of magnetic centers in bearingless switched reluctance motors is proposed for vibration reduction. For that purpose, the theoretical formulae of the magnetic attraction force can be derived with an assumption of simple permeance distribution. It is confirmed with the two-dimensional finite element analysis that the theoretical formulae are very close to the analysis results of magnetic attraction force. It is shown in experimental results that the vibration reduction of radial displacements can be realized by using the proposed feed-forward compensator. In addition, the proposed feed forward compensator is found to be also effective for radial vibration suppression in general switched reluctance motors supported by mechanical bearings.

REFERENCES

[1] C. A. Ferreira. S. R. Jones, W. S. Heglund, and W. D. Jones, “Detailed design of a 30-kW switched reluctance starter/generator system for a gas turbine engine application,” IEEE Trans. on Industry Applications, Vol. 31, pp. 553-561, 1995.

[2] T. J. E. Miller, “Faults and unbalance forces in the switched reluctance machine,” IEEE Trans. on Industry Applications, Vol. 31, pp. 319-328, 1995.

[3] M. Takemoto, A. Chiba, and T. Fukao, "A New Control Method of Bearingless Switched Reluctance Motors Using Square-wave Currents," Proceedings of the 2000 IEEE Power Engineering Society Winter Meeting, CD-ROM, January 2000.

[4] M. Takemoto, K. Shimada, A. Chiba, and T. Fukao, "A Design and Characteristics of Switched Reluctance Type Bearingless Motors," 4th International Symposium on Magnetic Suspension Technology, NASA/CP-1998-207654, pp. 49-63, May 1998.

[5] M. Takemoto, A. Chiba, and T. Fukao, "Compensation of Unbalanced Magnetic Attraction and Vibration Suppression of Bearingless Switched Reluctance Motors," 2000 National Convention Record of the IEE Japan, No.5-127, pp. 2097-2098, 2000 (in Japanese).